FERMILAB-PUB-11-015-E

Measurement of the Top Quark Mass in the Lepton+Jets Channel Using the Lepton Transverse Momentum

T. Aaltonen,[21] B. Álvarez González[v],[9] S. Amerio,[41] D. Amidei,[32] A. Anastassov,[36] A. Annovi,[17] J. Antos,[12] G. Apollinari,[15] J.A. Appel,[15] A. Apresyan,[46] T. Arisawa,[56] A. Artikov,[13] J. Asaadi,[51] W. Ashmanskas,[15] B. Auerbach,[59] A. Aurisano,[51] F. Azfar,[40] W. Badgett,[15] A. Barbaro-Galtieri,[26] V.E. Barnes,[46] B.A. Barnett,[23] P. Barria[cc],[44] P. Bartos,[12] M. Bauce[aa],[41] G. Bauer,[30] F. Bedeschi,[44] D. Beecher,[28] S. Behari,[23] G. Bellettini[bb],[44] J. Bellinger,[58] D. Benjamin,[14] A. Beretvas,[15] A. Bhatti,[48] M. Binkley*,[15] D. Bisello[aa],[41] I. Bizjak[gg],[28] K.R. Bland,[5] B. Blumenfeld,[23] A. Bocci,[14] A. Bodek,[47] D. Bortoletto,[46] J. Boudreau,[45] A. Boveia,[11] B. Brau[a],[15] L. Brigliadori[z],[6] A. Brisuda,[12] C. Bromberg,[33] E. Brucken,[21] M. Bucciantonio[bb],[44] J. Budagov,[13] H.S. Budd,[47] S. Budd,[22] K. Burkett,[15] G. Busetto[aa],[41] P. Bussey,[19] A. Buzatu,[31] C. Calancha,[29] S. Camarda,[4] M. Campanelli,[33] M. Campbell,[32] F. Canelli[12],[15] A. Canepa,[43] B. Carls,[22] D. Carlsmith,[58] R. Carosi,[44] S. Carrillo[k],[16] S. Carron,[15] B. Casal,[9] M. Casarsa,[15] A. Castro[z],[6] P. Catastini,[15] D. Cauz,[52] V. Cavaliere[cc],[44] M. Cavalli-Sforza,[4] A. Cerri[f],[26] L. Cerrito[q],[28] Y.C. Chen,[1] M. Chertok,[7] G. Chiarelli,[44] G. Chlachidze,[15] F. Chlebana,[15] K. Cho,[25] D. Chokheli,[13] J.P. Chou,[20] W.H. Chung,[58] Y.S. Chung,[47] C.I. Ciobanu,[42] M.A. Ciocci[cc],[44] A. Clark,[18] G. Compostella[aa],[41] M.E. Convery,[15] J. Conway,[7] M.Corbo,[42] M. Cordelli,[17] C.A. Cox,[7] D.J. Cox,[7] F. Crescioli[bb],[44] C. Cuenca Almenar,[59] J. Cuevas[v],[9] R. Culbertson,[15] D. Dagenhart,[15] N. d'Ascenzo[t],[42] M. Datta,[15] P. de Barbaro,[47] S. De Cecco,[49] G. De Lorenzo,[4] M. Dell'Orso[bb],[44] C. Deluca,[4] L. Demortier,[48] J. Deng[c],[14] M. Deninno,[6] F. Devoto,[21] M. d'Errico[aa],[41] A. Di Canto[bb],[44] B. Di Ruzza,[44] J.R. Dittmann,[5] M. D'Onofrio,[27] S. Donati[bb],[44] P. Dong,[15] M. Dorigo,[52] T. Dorigo,[41] K. Ebina,[56] A. Elagin,[51] A. Eppig,[32] R. Erbacher,[7] D. Errede,[22] S. Errede,[22] N. Ershaidat[y],[42] R. Eusebi,[51] H.C. Fang,[26] S. Farrington,[40] M. Feindt,[24] J.P. Fernandez,[29] C. Ferrazza[dd],[44] R. Field,[16] G. Flanagan[r],[46] R. Forrest,[7] M.J. Frank,[5] M. Franklin,[20] J.C. Freeman,[15] Y. Funakoshi,[56] I. Furic,[16] M. Gallinaro,[48] J. Galyardt,[10] J.E. Garcia,[18] A.F. Garfinkel,[46] P. Garosi[cc],[44] H. Gerberich,[22] E. Gerchtein,[15] S. Giagu[ee],[49] V. Giakoumopoulou,[3] P. Giannetti,[44] K. Gibson,[45] C.M. Ginsburg,[15] N. Giokaris,[3] P. Giromini,[17] M. Giunta,[44] G. Giurgiu,[23] V. Glagolev,[13] D. Glenzinski,[15] M. Gold,[35] D. Goldin,[51] N. Goldschmidt,[16] A. Golossanov,[15] G. Gomez,[9] G. Gomez-Ceballos,[30] M. Goncharov,[30] O. González,[29] I. Gorelov,[35] A.T. Goshaw,[14] K. Goulianos,[48] A. Gresele,[41] S. Grinstein,[4] C. Grosso-Pilcher,[11] R.C. Group,[55] J. Guimaraes da Costa,[20] Z. Gunay-Unalan,[33] C. Haber,[26] S.R. Hahn,[15] E. Halkiadakis,[50] A. Hamaguchi,[39] J.Y. Han,[47] F. Happacher,[17] K. Hara,[53] D. Hare,[50] M. Hare,[54] R.F. Harr,[57] K. Hatakeyama,[5] C. Hays,[40] M. Heck,[24] J. Heinrich,[43] M. Herndon,[58] S. Hewamanage,[5] D. Hidas,[50] A. Hocker,[15] W. Hopkins[g],[15] D. Horn,[24] S. Hou,[1] R.E. Hughes,[37] M. Hurwitz,[11] U. Husemann,[59] N. Hussain,[31] M. Hussein,[33] J. Huston,[33] G. Introzzi,[44] M. Iori[ee],[49] A. Ivanov[o],[7] E. James,[15] D. Jang,[10] B. Jayatilaka,[14] E.J. Jeon,[25] M.K. Jha,[6] S. Jindariani,[15] W. Johnson,[7] M. Jones,[46] K.K. Joo,[25] S.Y. Jun,[10] T.R. Junk,[15] T. Kamon,[51] P.E. Karchin,[57] Y. Kato[n],[39] W. Ketchum,[11] J. Keung,[43] V. Khotilovich,[51] B. Kilminster,[15] D.H. Kim,[25] H.S. Kim,[25] H.W. Kim,[25] J.E. Kim,[25] M.J. Kim,[17] S.B. Kim,[25] S.H. Kim,[53] Y.K. Kim,[11] N. Kimura,[56] M. Kirby,[15] S. Klimenko,[16] K. Kondo,[56] D.J. Kong,[25] J. Konigsberg,[16] A.V. Kotwal,[14] M. Kreps,[24] J. Kroll,[43] D. Krop,[11] N. Krumnack[l],[5] M. Kruse,[14] V. Krutelyov[d],[51] T. Kuhr,[24] M. Kurata,[53] S. Kwang,[11] A.T. Laasanen,[46] S. Lami,[44] S. Lammel,[15] M. Lancaster,[28] R.L. Lander,[7] K. Lannon[u],[37] A. Lath,[50] G. Latino[cc],[44] I. Lazzizzera,[41] T. LeCompte,[2] E. Lee,[51] H.S. Lee,[11] J.S. Lee,[25] S.W. Lee[w],[51] S. Leo[bb],[44] S. Leone,[44] J.D. Lewis,[15] C.-J. Lin,[26] J. Linacre,[40] M. Lindgren,[15] E. Lipeles,[43] A. Lister,[18] D.O. Litvintsev,[15] C. Liu,[45] Q. Liu,[46] T. Liu,[15] S. Lockwitz,[59] N.S. Lockyer,[43] A. Loginov,[59] D. Lucchesi[aa],[41] J. Lueck,[24] P. Lujan,[26] P. Lukens,[15] G. Lungu,[48] J. Lys,[26] R. Lysak,[12] R. Madrak,[15] K. Maeshima,[15] K. Makhoul,[30] P. Maksimovic,[23] S. Malik,[48] G. Manca[b],[27] A. Manousakis-Katsikakis,[3] F. Margaroli,[46] C. Marino,[24] M. Martínez,[4] R. Martínez-Ballarín,[29] P. Mastrandrea,[49] M. Mathis,[23] M.E. Mattson,[57] P. Mazzanti,[6] K.S. McFarland,[47] P. McIntyre,[51] R. McNulty[i],[27] A. Mehta,[27] P. Mehtala,[21] A. Menzione,[44] C. Mesropian,[48] T. Miao,[15] D. Mietlicki,[32] A. Mitra,[1] H. Miyake,[53] S. Moed,[20] N. Moggi,[6] M.N. Mondragon[k],[15] C.S. Moon,[25] R. Moore,[15] M.J. Morello,[15] J. Morlock,[24] P. Movilla Fernandez,[15] A. Mukherjee,[15] Th. Muller,[24] P. Murat,[15] M. Mussini[z],[6] J. Nachtman[m],[15] Y. Nagai,[53] J. Naganoma,[56] I. Nakano,[38] A. Napier,[54] J. Nett,[51] C. Neu,[55] M.S. Neubauer,[22] J. Nielsen[e],[26] L. Nodulman,[2] O. Norniella,[22] E. Nurse,[28] L. Oakes,[40] S.H. Oh,[14] Y.D. Oh,[25] I. Oksuzian,[55] T. Okusawa,[39] R. Orava,[21] L. Ortolan,[4] S. Pagan Griso[aa],[41] C. Pagliarone,[52] E. Palencia[f],[9] V. Papadimitriou,[15] A.A. Paramonov,[2] J. Patrick,[15] G. Pauletta[ff],[52] M. Paulini,[10] C. Paus,[30] D.E. Pellett,[7] A. Penzo,[52] T.J. Phillips,[14] G. Piacentino,[44] E. Pianori,[43] J. Pilot,[37] K. Pitts,[22] C. Plager,[8] L. Pondrom,[58] K. Potamianos,[46] O. Poukhov*,[13] F. Prokoshin[x],[13] A. Pronko,[15] F. Ptohos[h],[17] E. Pueschel,[10] G. Punzi[bb],[44] J. Pursley,[58] A. Rahaman,[45] V. Ramakrishnan,[58] N. Ranjan,[46] I. Redondo,[29] P. Renton,[40] M. Rescigno,[49] F. Rimondi[z],[6] L. Ristori[45],[15] A. Robson,[19]

Operated by Fermi Research Alliance, LLC under Contract No. DE-AC02-07CH11359 with the United States Department of Energy

T. Rodrigo,[9] T. Rodriguez,[43] E. Rogers,[22] S. Rolli,[54] R. Roser,[15] M. Rossi,[52] F. Rubbo,[15] F. Ruffini[cc],[44] A. Ruiz,[9] J. Russ,[10] V. Rusu,[15] A. Safonov,[51] W.K. Sakumoto,[47] Y. Sakurai,[56] L. Santi[ff],[52] L. Sartori,[44] K. Sato,[53] V. Saveliev[t],[42] A. Savoy-Navarro,[42] P. Schlabach,[15] A. Schmidt,[24] E.E. Schmidt,[15] M.P. Schmidt[*],[59] M. Schmitt,[36] T. Schwarz,[7] L. Scodellaro,[9] A. Scribano[cc],[44] F. Scuri,[44] A. Sedov,[46] S. Seidel,[35] Y. Seiya,[39] A. Semenov,[13] F. Sforza[bb],[44] A. Sfyrla,[22] S.Z. Shalhout,[7] T. Shears,[27] P.F. Shepard,[45] M. Shimojima[s],[53] S. Shiraishi,[11] M. Shochet,[11] I. Shreyber,[34] A. Simonenko,[13] P. Sinervo,[31] A. Sissakian[*],[13] K. Sliwa,[54] J.R. Smith,[7] F.D. Snider,[15] A. Soha,[15] S. Somalwar,[50] V. Sorin,[4] P. Squillacioti,[15] M. Stancari,[15] M. Stanitzki,[59] R. St. Denis,[19] B. Stelzer,[31] O. Stelzer-Chilton,[31] D. Stentz,[36] J. Strologas,[35] G.L. Strycker,[32] Y. Sudo,[53] A. Sukhanov,[16] I. Suslov,[13] K. Takemasa,[53] Y. Takeuchi,[53] J. Tang,[11] M. Tecchio,[32] P.K. Teng,[1] J. Thom[g],[15] J. Thome,[10] G.A. Thompson,[22] E. Thomson,[43] P. Ttito-Guzmán,[29] S. Tkaczyk,[15] D. Toback,[51] S. Tokar,[12] K. Tollefson,[33] T. Tomura,[53] D. Tonelli,[15] S. Torre,[17] D. Torretta,[15] P. Totaro[ff],[52] M. Trovato[dd],[44] Y. Tu,[43] F. Ukegawa,[53] S. Uozumi,[25] A. Varganov,[32] F. Vázquez[k],[16] G. Velev,[15] C. Vellidis,[3] M. Vidal,[29] I. Vila,[9] R. Vilar,[9] J. Vizán,[9] M. Vogel,[35] G. Volpi[bb],[44] P. Wagner,[43] R.L. Wagner,[15] T. Wakisaka,[39] R. Wallny,[8] S.M. Wang,[1] A. Warburton,[31] D. Waters,[28] M. Weinberger,[51] W.C. Wester III,[15] B. Whitehouse,[54] D. Whiteson[c],[43] A.B. Wicklund,[2] E. Wicklund,[15] S. Wilbur,[11] F. Wick,[24] H.H. Williams,[43] J.S. Wilson,[37] P. Wilson,[15] B.L. Winer,[37] P. Wittich[g],[15] S. Wolbers,[15] H. Wolfe,[37] T. Wright,[32] X. Wu,[18] Z. Wu,[5] K. Yamamoto,[39] J. Yamaoka,[14] T. Yang,[15] U.K. Yang[p],[11] Y.C. Yang,[25] W.-M. Yao,[26] G.P. Yeh,[15] K. Yi[m],[15] J. Yoh,[15] K. Yorita,[56] T. Yoshida[j],[39] G.B. Yu,[14] I. Yu,[25] S.S. Yu,[15] J.C. Yun,[15] A. Zanetti,[52] Y. Zeng,[14] and S. Zucchelli[z6]

(CDF Collaboration[†])

[1]*Institute of Physics, Academia Sinica, Taipei, Taiwan 11529, Republic of China*
[2]*Argonne National Laboratory, Argonne, Illinois 60439, USA*
[3]*University of Athens, 157 71 Athens, Greece*
[4]*Institut de Fisica d'Altes Energies, ICREA, Universitat Autonoma de Barcelona, E-08193, Bellaterra (Barcelona), Spain*
[5]*Baylor University, Waco, Texas 76798, USA*
[6]*Istituto Nazionale di Fisica Nucleare Bologna, [z]University of Bologna, I-40127 Bologna, Italy*
[7]*University of California, Davis, Davis, California 95616, USA*
[8]*University of California, Los Angeles, Los Angeles, California 90024, USA*
[9]*Instituto de Fisica de Cantabria, CSIC-University of Cantabria, 39005 Santander, Spain*
[10]*Carnegie Mellon University, Pittsburgh, Pennsylvania 15213, USA*
[11]*Enrico Fermi Institute, University of Chicago, Chicago, Illinois 60637, USA*
[12]*Comenius University, 842 48 Bratislava, Slovakia; Institute of Experimental Physics, 040 01 Kosice, Slovakia*
[13]*Joint Institute for Nuclear Research, RU-141980 Dubna, Russia*
[14]*Duke University, Durham, North Carolina 27708, USA*
[15]*Fermi National Accelerator Laboratory, Batavia, Illinois 60510, USA*
[16]*University of Florida, Gainesville, Florida 32611, USA*
[17]*Laboratori Nazionali di Frascati, Istituto Nazionale di Fisica Nucleare, I-00044 Frascati, Italy*
[18]*University of Geneva, CH-1211 Geneva 4, Switzerland*
[19]*Glasgow University, Glasgow G12 8QQ, United Kingdom*
[20]*Harvard University, Cambridge, Massachusetts 02138, USA*
[21]*Division of High Energy Physics, Department of Physics, University of Helsinki and Helsinki Institute of Physics, FIN-00014, Helsinki, Finland*
[22]*University of Illinois, Urbana, Illinois 61801, USA*
[23]*The Johns Hopkins University, Baltimore, Maryland 21218, USA*
[24]*Institut für Experimentelle Kernphysik, Karlsruhe Institute of Technology, D-76131 Karlsruhe, Germany*
[25]*Center for High Energy Physics: Kyungpook National University, Daegu 702-701, Korea; Seoul National University, Seoul 151-742, Korea; Sungkyunkwan University, Suwon 440-746, Korea; Korea Institute of Science and Technology Information, Daejeon 305-806, Korea; Chonnam National University, Gwangju 500-757, Korea; Chonbuk National University, Jeonju 561-756, Korea*
[26]*Ernest Orlando Lawrence Berkeley National Laboratory, Berkeley, California 94720, USA*
[27]*University of Liverpool, Liverpool L69 7ZE, United Kingdom*
[28]*University College London, London WC1E 6BT, United Kingdom*
[29]*Centro de Investigaciones Energeticas Medioambientales y Tecnologicas, E-28040 Madrid, Spain*
[30]*Massachusetts Institute of Technology, Cambridge, Massachusetts 02139, USA*
[31]*Institute of Particle Physics: McGill University, Montréal, Québec, Canada H3A 2T8; Simon Fraser University, Burnaby, British Columbia, Canada V5A 1S6; University of Toronto, Toronto, Ontario, Canada M5S 1A7; and TRIUMF, Vancouver, British Columbia, Canada V6T 2A3*
[32]*University of Michigan, Ann Arbor, Michigan 48109, USA*

[33]Michigan State University, East Lansing, Michigan 48824, USA
[34]Institution for Theoretical and Experimental Physics, ITEP, Moscow 117259, Russia
[35]University of New Mexico, Albuquerque, New Mexico 87131, USA
[36]Northwestern University, Evanston, Illinois 60208, USA
[37]The Ohio State University, Columbus, Ohio 43210, USA
[38]Okayama University, Okayama 700-8530, Japan
[39]Osaka City University, Osaka 588, Japan
[40]University of Oxford, Oxford OX1 3RH, United Kingdom
[41]Istituto Nazionale di Fisica Nucleare, Sezione di Padova-Trento, [aa]University of Padova, I-35131 Padova, Italy
[42]LPNHE, Universite Pierre et Marie Curie/IN2P3-CNRS, UMR7585, Paris, F-75252 France
[43]University of Pennsylvania, Philadelphia, Pennsylvania 19104, USA
[44]Istituto Nazionale di Fisica Nucleare Pisa, [bb]University of Pisa,
[cc]University of Siena and [dd]Scuola Normale Superiore, I-56127 Pisa, Italy
[45]University of Pittsburgh, Pittsburgh, Pennsylvania 15260, USA
[46]Purdue University, West Lafayette, Indiana 47907, USA
[47]University of Rochester, Rochester, New York 14627, USA
[48]The Rockefeller University, New York, New York 10065, USA
[49]Istituto Nazionale di Fisica Nucleare, Sezione di Roma 1,
[ee]Sapienza Università di Roma, I-00185 Roma, Italy
[50]Rutgers University, Piscataway, New Jersey 08855, USA
[51]Texas A&M University, College Station, Texas 77843, USA
[52]Istituto Nazionale di Fisica Nucleare Trieste/Udine,
I-34100 Trieste, [ff]University of Trieste/Udine, I-33100 Udine, Italy
[53]University of Tsukuba, Tsukuba, Ibaraki 305, Japan
[54]Tufts University, Medford, Massachusetts 02155, USA
[55]University of Virginia, Charlottesville, VA 22906, USA
[56]Waseda University, Tokyo 169, Japan
[57]Wayne State University, Detroit, Michigan 48201, USA
[58]University of Wisconsin, Madison, Wisconsin 53706, USA
[59]Yale University, New Haven, Connecticut 06520, USA

(Dated: January 24, 2011)

This letter reports a measurement of the top quark mass, M_{top}, in data from $p\bar{p}$ collisions at $\sqrt{s} = 1.96$ TeV corresponding to 2.7 fb^{-1} of integrated luminosity at the Fermilab Tevatron using the CDF II detector. Events with the lepton+jets topology are selected. An unbinned likelihood is constructed based on the dependence of the lepton transverse momentum, $P_{\rm T}$, on M_{top}. A maximum likelihood fit to the data yields a measured mass $M_{top} = 176.9 \pm 8.0_{\rm stat} \pm 2.7_{\rm syst}$ GeV/c^2. In this measurement, the contribution by the jet energy scale uncertainty to the systematic error is negligible. The result provides an important consistency test for other M_{top} measurements where explicit use of the jet energy is made for deriving the top quark mass.

I. INTRODUCTION

The top quark is the heaviest known fundamental particle. Since the discovery of this particle in 1995 at the Fermilab Tevatron [1], both the CDF and D0 experiments have been improving the precision of the measurement of its mass M_{top}, which is a fundamental parameter in the Standard Model (SM) of particle physics. Loop corrections in electroweak theory relate M_{top} and the W boson mass M_W to the mass of the predicted Higgs boson [2]. Therefore, precision measurements of M_{top} provide constraints on the value of the Higgs boson mass as well as a consistency check of the SM electroweak theory [3].

The largest systematic uncertainties in the measure-

*Deceased
†With visitors from [a]University of Massachusetts Amherst, Amherst, Massachusetts 01003, [b]Istituto Nazionale di Fisica Nucleare, Sezione di Cagliari, 09042 Monserrato (Cagliari), Italy, [c]University of California Irvine, Irvine, CA 92697, [d]University of California Santa Barbara, Santa Barbara, CA 93106 [e]University of California Santa Cruz, Santa Cruz, CA 95064, [f]CERN,CH-1211 Geneva, Switzerland, [g]Cornell University, Ithaca, NY 14853, [h]University of Cyprus, Nicosia CY-1678, Cyprus, [i]University College Dublin, Dublin 4, Ireland, [j]University of Fukui, Fukui City, Fukui Prefecture, Japan 910-0017, [k]Universidad Iberoamericana, Mexico D.F., Mexico, [l]Iowa State University, Ames, IA 50011, [m]University of Iowa, Iowa City, IA 52242, [n]Kinki University, Higashi-Osaka City, Japan 577-8502, [o]Kansas State University, Manhattan, KS 66506, [p]University of Manchester, Manchester M13 9PL, England, [q]Queen Mary, University of London, London, E1 4NS, England, [r]Muons, Inc., Batavia, IL 60510, [s]Nagasaki Institute of Applied Science, Nagasaki, Japan, [t]National Research Nuclear University, Moscow, Russia, [u]University of Notre Dame, Notre Dame, IN 46556, [v]Universidad de Oviedo, E-33007 Oviedo, Spain, [w]Texas Tech University, Lubbock, TX 79609, [x]Universidad Tecnica Federico Santa Maria, 110v Valparaiso, Chile, [y]Yarmouk University, Irbid 211-63, Jordan, [gg]On leave from J. Stefan Institute, Ljubljana, Slovenia,

ment of M_{top} are due to uncertainties in the measurement of jets. Jets are composite objects which must be associated with the partons produced in $t\bar{t}$ decays using jet-parton combinatorics and energy transfer functions derived from Monte Carlo (MC) simulation. Measuring the jet energy requires detailed corrections and an overall scale calibration. The *in situ* energy scale calibration with a W mass constraint used in other M_{top} measurement techniques [4] is not directly applicable to jets produced by b quarks. On the other hand, charged leptons (electrons or muons) produced in $t\bar{t}$ decays are directly observable in the detector and their momenta can be measured with very high precision. Leptons thus provide a very clean probe of the kinematics of $t\bar{t}$ decays. The sensitivity of their momentum on the top quark mass can be used to measure M_{top} without the complexities and related uncertainties which are inherent to the use of jets, albeit with less statistical precision. The result reported in this letter is, therefore, complementary to the existing precision measurements by having different systematic uncertainties than the previously published results.

In $p\bar{p}$ collisions, top quarks are produced predominantly as $t\bar{t}$ pairs. Within the SM, the top quark decays almost exlusively into a W boson and a bottom quark b [5]. The events in which one of the W bosons decays leptonically to a charged lepton and a neutrino and the other decays hadronically into two jets define the "lepton+jets" decay channel, $t\bar{t} \rightarrow W^+bW^-\bar{b} \rightarrow l\nu_l bq\bar{q}'\bar{b}$. Including the two jets arising from the b quarks, the lepton+jets topology contains at least four jets. Additional jets may be generated from gluon radiation or from soft hadron interactions forming the "underlying event". Despite this complication, the lepton+jets channel provides the best balance of available statistics and sample purity.

The sensitivity of kinematic variables of the lepton to M_{top} has to be studied using a MC model of $t\bar{t}$ events. In a preliminary study of the possibility of using only leptons to measure M_{top} it was found that the optimum variable to use is the lepton transverse momentum $P_{\rm T}$ [6]. This variable is generically used to signify the transverse momentum of muons measured in the tracker or the transverse energy of electrons measured in the calorimeter [7], which offers better resolution than the tracker for high energy electrons.

The only previous analysis using the transverse momentum of leptons with data of 1.9 fb^{-1} integrated luminosity from the CDF experiment [8] explored the mean value of the lepton $P_{\rm T}$. That analysis also exploited the mean value of the transverse path length of b-flavored hadrons produced in $t\bar{t}$ decays and combined the two results to measure M_{top} in the lepton+jets channel of $t\bar{t}$ decays. In the measurement reported in this letter a shape analysis of the lepton $P_{\rm T}$ spectrum is applied in the same decay channel. This technique is less sensitive to acceptance related effects, which alter the mean value of the lepton $P_{\rm T}$ but leave the shape of the $P_{\rm T}$ distribution unchanged, and thus allows for a measurement with smaller systematic uncertainties.

TABLE I: Expected and observed lepton + $\geq$4 jets sample for an integrated luminosity of 2.7 fb^{-1}. The $t\bar{t}$ contribution is estimated using a cross section of 6.7 pb [18] and $M_{top} = 175$ GeV/c^2. The uncertainties are statistical only.

Event type	Expected number of events
W+heavy flavor	91.3±15.6
W+light flavor	29.6±6.0
$Z \rightarrow ll$+jets	5.3±1.3
Dibosons (WW, WZ, ZZ)	8.6±1.5
Single top	8.6±1.2
Fakes	34.9±22.5
Total background	178.8±28.2
$t\bar{t}$ signal	634.9±44.8
Total expectation	813.8±53.0
Observed events	858

II. DETECTOR AND EVENT SELECTION

The measurement described in this letter uses data collected with the Collider Detector at Fermilab (CDF) II detector [9] at the Tevatron $p\bar{p}$ collider corresponding to an integrated luminosity of 2.7 fb^{-1}. CDF is a cylindrically symmetric detector surrounding the colliding beams. It consists, radially from inside to outside, of an inner silicon tracker allowing for accurate vertex reconstruction and an outer wire chamber tracker, both operating in a uniform magnetic field of 1.4 Tesla which is produced by a superconducting solenoid surrounding the tracker; scintillators for time-of-flight measurements; a sampling calorimeter with an inner electromagnetic compartment and an outer hadronic compartment; and wire chambers for muon identification. The tracking system measures charged particle tracks with a transverse momentum precision of $\Delta P_{\rm T}/P_{\rm T}^2 = 0.07\%(\mathrm{GeV}/c)^{-1}$. The central calorimeters have an electromagnetic (hadronic) energy resolution of $\sigma(E_{\rm T})/E_{\rm T} \sim 13.5\%/\sqrt{E_{\rm T}(\mathrm{GeV})} \oplus 1.5\%$ ($\sigma(E_{\rm T})/E_{\rm T} \sim 50\%/\sqrt{E_{\rm T}(\mathrm{GeV})} \oplus 3\%$) and a tower segmentation of $\Delta\eta \times \Delta\phi \simeq 0.1 \times 15°$.

The leptons used in this measurement were detected in the central region of the CDF detector, covering a pseudorapidity range of $|\eta| \leq 1$ [7], with an inclusive lepton trigger requiring an electron with $E_{\rm T} \geq 18$ GeV or a muon with $P_{\rm T} \geq 18$ GeV/c. From this inclusive lepton dataset, events are selected offline in the lepton+jets channel by requiring one electron with transverse energy $E_{\rm T} \geq 20$ GeV or one muon with transverse momentum $P_{\rm T} \geq 20$ GeV/c, at least four jets with transverse energy $E_{\rm T} \geq 20$ GeV and pseudorapidity $|\eta| \leq 2$, and missing transverse energy $\not\!\!E_{\rm T} \geq 20$ GeV [10] to account for the unobserved neutrino. Electrons are reconstructed as

isolated energy clusters in the electromagnetic calorimeter [11] and matched to tracks fiducial to these clusters. Muons are reconstructed from tracks fiducial to the muon chambers, matched to isolated tracks in the central tracker, and are required to deposit minimal energy in the calorimeter. Jets are reconstructed as energy clusters in the hadronic calorimeter towers within a cone of radius 0.4 [11] around a seed tower. Jet energies are corrected for non-uniformities in the calorimeter response as a function of the jet pseudorapidity, for multiple $p\bar{p}$ interactions in the event, and for the energy scale of the calorimeter [12]. The expected fraction of $t\bar{t}$ lepton+jets events passing the above selection requirements is approximately 10%. The signal to background fraction is S/B$\sim$0.5. To enhance this fraction, at least one jet is required to be tagged as originating from a heavy flavor quark using a secondary vertex tagging algorithm [13]. The fraction of signal events passing this additional requirement is reduced to $\sim$6%, while S/B rises to $\sim$3.7. Decays of the W boson to a τ lepton which subsequently decays to an electron or muon can also pass all selction requirements and they amount to approximately 7% of the $t\bar{t}$ signal.

III. BACKGROUND ESTIMATION

Background events from other SM processes passing the selection criteria contain: W boson production associated with jets from heavy flavor quarks ($b\bar{b}$, $c\bar{c}$ or c); W boson production associated with jets from light flavor quarks; Z boson production associated with jets where the Z decays leptonically and one lepton escapes detection, thus giving rise to high $\not\!\!E_{\rm T}$; diboson events (WW, WZ, ZZ) in which one boson decays leptonically and the other hadronically; single-top events where the W boson produced by the top quark decays leptonically; and events having a jet misidentified as a lepton, subsequently referred to as a "fake" lepton. The $t\bar{t}$ and diboson events were modeled using the PYTHIA generator [14]. The W+jets and Z+jets events were modeled using the ALPGEN generator [15] with the parton hadronization done by PYTHIA. The single top events were modeled using the MADGRAPH/MADEVENT generator [16] with the parton hadronization done again by PYTHIA. The modeled events were processed through the detector and trigger simuation and reconstructed using the CDF II software [17]. The $P_{\rm T}$ distribution of fake leptons was modeled using a data sample selected by requiring each event to fail at least one of the criteria of good lepton selection. The complete sample composition was estimated with a method used for the $t\bar{t}$ cross section measurement [18]. In this method the expected rates of $t\bar{t}$, Z+jets, diboson and single-top events are estimated from the MC; the rate of W+heavy-flavored jet events is estimated from the MC, adjusted to the data in the 1- and 2-jet control bins using a neural network; the rate of W+light-flavored jet events is estimated from the MC normalized to the rate of mis-tagged jet events in the data; and the rate of events with a fake lepton is estimated by fitting the total MC + fake leptons $\not\!\!E_{\rm T}$ spectrum to the $\not\!\!E_{\rm T}$ spectrum of the data.

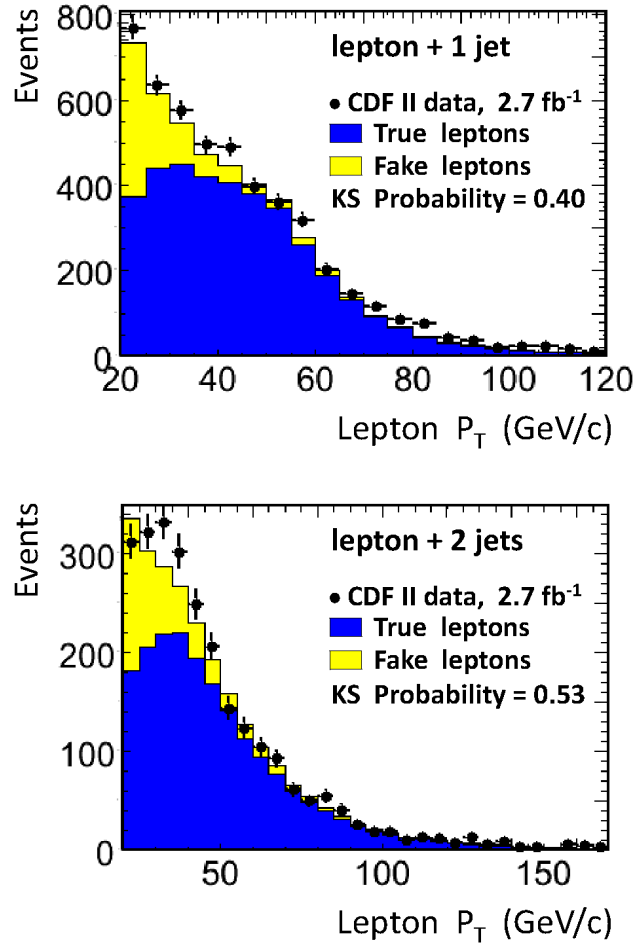

FIG. 1: Comparison of the expectations with the data in the lepton + 1 jet and lepton + 2 jets samples.

The total expected composition of the selected events is shown in Table I. Extensive validation tests of the background model were made in the control samples of events with one lepton and one or two jets, where the $t\bar{t}$ signal is expected to be negligible. Comparisons of the expectations with the data in the control samples are shown in Figure 1. Only shape discrepancies are of concern for the purpose of this measurement because the background normalization is varied in the fit to the data, as described in Section IV. There is a possible shape discrepancy between the total expectation and the data in the lepton + 2 jets control sample for $P_{\rm T} < 50$ GeV/c, attributed to the fake lepton shape being inaccurate. A systematic uncertainty from the fakes distribution is assigned to the final M_{top} measurement, as discussed in Section VI.

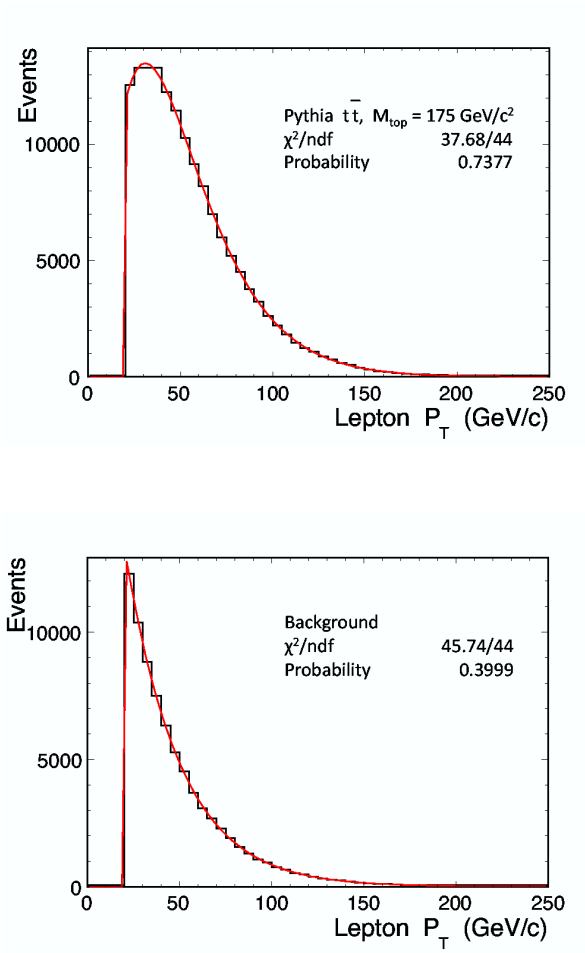

FIG. 2: **Top:** The fit of the incomplete Γ function to the PYTHIA lepton $P_{\rm T}$ histogram with input M_{top} = 175 GeV/c^2. **Bottom:** The fit of the incomplete Γ function to the lepton $P_{\rm T}$ histogram of the estimated total background.

IV. METHOD

A set of 27 PYTHIA $t\bar{t}$ samples with different central input M_{top} values between 150 and 200 GeV/c^2 was analyzed. The lepton $P_{\rm T}$ histograms of the selected events from each sample were constructed for each central M_{top} input value. Rather than using directly these histograms as binned templates to fit M_{top}, an analytical parametrization of the lepton $P_{\rm T}$ distribution is chosen for this measurement. All the lepton $P_{\rm T}$ histograms can be accurately modeled by the number of leptons N in the histogram times an incomplete Γ probability density function:

$$F\left(P_{\rm T};\, p, q\right) \;=\; \frac{1/q}{\Gamma(1+p, c/q)} \left(\frac{P_{\rm T}}{q}\right)^{p} \frac{e^{-P_{\rm T}/q}}{1+e^{(c-P_{\rm T})/a}}, \quad a,\, c,\, p,\, q > 0, \tag{1}$$

TABLE II: Fit parameters of the lepton $P_{\rm T}$ distribution model for the $t\bar{t}$ signal ($\alpha_{1,2,3,4}$) and for the total background ($\beta_{1,2}$).

Parameter		Value
Intercept	α_1	1.72±0.10
Slope	α_2 [(GeV/c)$^{-1}$]	−0.0009±0.0004
Intercept	α_3 [GeV/c]	6.19±0.26
Slope	α_4	0.079±0.001
	β_1	0.27±0.54
	β_2 [GeV/c]	26.73±6.79

with two free parameters p and q. The Fermi-Dirac factor $1/[1+e^{(c-P_{\rm T})/a}]$ gives a finite width a to the event selection threshold at $c = 20$ GeV/c and tends to a unit step function $\vartheta(c-P_{\rm T})$ in the limit of $a \to 0$ of the true, infinitely sharp lepton $P_{\rm T}$ cut. The fit of this function to any of the lepton $P_{\rm T}$ templates was insensitive to any choice of $a \leq 0.1$ GeV/c, while the χ^2 was progressively increasing for $a > 0.1$ GeV/c. This parameter was thus fixed at $a = 0.1$ GeV/c in the incomplete Γ function. An example of the fit of this function to the lepton $P_{\rm T}$ template with input $M_{top} = 175$ GeV/c^2 is shown in the top plot of Figure 2. The dependence of the lepton $P_{\rm T}$ distribution on the input M_{top} of the templates was studied by fitting p and q to each $t\bar{t}$ signal template. The fits are shown in the top plots of Figure 3. The parameter p shows significant local fluctuations because it is mostly sensitive to the location of the distribution's maximum which lies very close to the cut at 20 GeV/c. Therefore, the individual fit to each template does not constrain this parameter strongly enough. Apart from this the fits show an approximately linear dependence of both parameters on M_{top}. Based on this observation, the dependence was modeled by leading order Taylor expansions in terms of M_{top}:

$$p = \alpha_1 + \alpha_2 M_{top} \qquad q = \alpha_3 + \alpha_4 M_{top}, \tag{2}$$

where terms of $O(M_{top}^2)$ were dropped. The zeroth and first order coefficients $\alpha_{1,2,3,4}$ were determined from a fit of Equations 1 and 2 to all $t\bar{t}$ signal templates simultaneously using the program MINUIT [19]. The simultaneous fit smooths out local fluctuations of the parameters, giving an imporved χ^2 probability. The results are shown in Table II. Coefficient α_1 is anti-correlated with α_2, and α_3 with α_4, at the level of 60% in either case, whereas other correlations are much smaller. This parameterization encapsulates all of the M_{top} information that the MC signal templates provide. The incomplete Γ function was also found to model accurately the total background template which is constructed by adding the lepton $P_{\rm T}$ histograms of all background contributions, according to the expected rates of Table I, and is independent of M_{top}. The fit of this function to the total background template

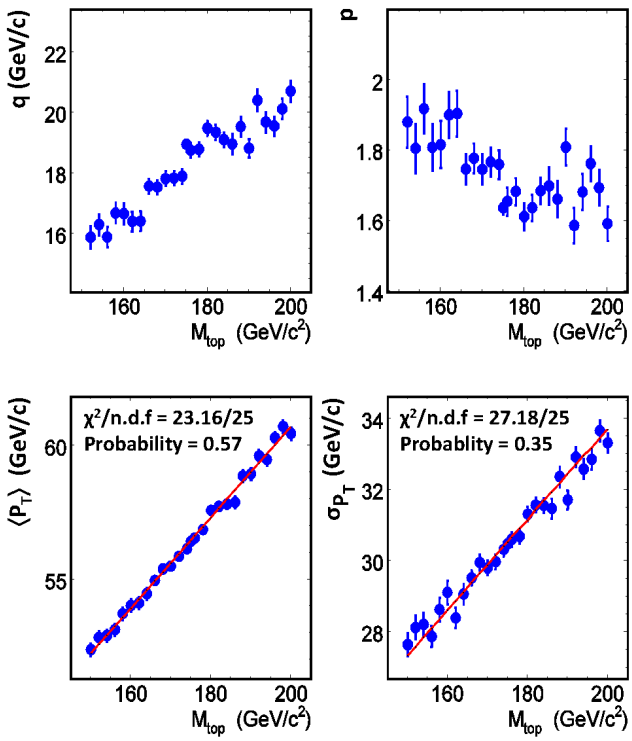

FIG. 3: **Top:** The parameters q (left) and p (right) of the lepton $P_{\rm T}$ distribution model as functions of the input M_{top} of the Monte Carlo signal templates. The plots show the linear trends of both parameters. **Bottom:** The mean (left) and standard deviation (right) of the templates as functions of the input M_{top} compared with the corresponding first two statistical moments of the lepton $P_{\rm T}$ distribution model (straight lines), computed using the slopes and intercepts of Table II. The χ^2 probabilities are calculated from the deviations of the points from the lines, without fitting, and are therefore measures of validity of the model.

is shown in the bottom plot of Figure 2. The background lepton $P_{\rm T}$ distribution was, therefore, modeled using the same constants $c = 20$ GeV/c and $a = 0.1$ GeV/c and fitting the free parameters p and q. The background fit values β_1 of p and β_2 of q are also shown in Table II. The model was validated by verifying that the first two statistical moments of both signal and background template histograms were reproduced, within statistical uncertainties, by the incomplete Γ function using the fit parameters of Table II. This is shown for the signal templates in the bottom plots of Figure 3, where the two moments computed directly from the templates are compared with the values obtained by integrating the incomplete Γ function. It is worth noting that the two moments depend linearly on M_{top} as well.

An unbinned likelihood, L, was constructed based on the modeling of the lepton $P_{\rm T}$ distributions for signal and background events:

$$L = \frac{1}{\sqrt{2\pi}\,\delta b}\exp\left[-\frac{1}{2}\left(\frac{n_b - b}{\delta b}\right)^2\right] \times \frac{(n_s+n_b)^N e^{-(n_s+n_b)}}{N!} \times \prod_{i=1}^{N}\frac{n_s\,F\left(P_{\rm T}^{(i)};\,\vec{\alpha};\,M_{top}\right) + n_b\,F\left(P_{\rm T}^{(i)};\,\vec{\beta}\right)}{n_s+n_b} \quad (3)$$

The likelihood contains the product of the normalized probabilities of n_s leptons to come from the $t\bar{t}$ signal and n_b leptons to come from the background. By fixing the shape parameters $\vec{\alpha} = (\alpha_1, \alpha_2, \alpha_3, \alpha_4)$ of the signal and $\vec{\beta} = (\beta_1, \beta_2)$ of the background to the values of Table II, the likelihood becomes a function of M_{top} and of the numbers n_s and n_b. It contains a Gaussian constraint relating n_b to the expected total number b of background leptons, with δb being the uncertainty of this number derived by adding quadratically the uncertainties of Table I, and a Poisson constraint relating the sum $n_s + n_b$ to the number N of observed leptons of Table I.

V. CORRECTIONS AND TESTS

A detailed calibration of the lepton $P_{\rm T}$ scale was performed. The overall scale was calibrated by tuning the reconstructed $Z \to e^+e^-$ and $Z \to \mu^+\mu^-$ mass peaks of the data and MC samples to the Z mass world average [5]. The correction applied to the electron $E_{\rm T}$ scale is $+0.4\%$ for the data and -0.4% for the MC. The correction to the muon $P_{\rm T}$ scale is $+0.4\%$ for the data, while no significant shift was found in the MC. The local muon $P_{\rm T}$ scale was calibrated by binning the data and MC samples in $1/P_{\rm T}$ and reconstructing the $Z \to \mu^+\mu^-$ mass peak in each bin. Local changes of the $P_{\rm T}$ scale were examined by tuning to the Z mass world average. The top plot of Figure 4 shows the relative change in the scale as a function of $1/P_{\rm T}$, which is proportional to the muon track curvature in the magnetic field of the detector. The fit of a constant term describes the points reasonably well, showing no significant local change in the $P_{\rm T}$ scale. The local electron $E_{\rm T}$ scale was calibrated by correcting the slope of the energy to momentum E/P ratio as a function of $E_{\rm T}$ of electron + 1 jet data and MC samples, from which an $E_{\rm T}$-dependent correction was derived. The E/P ratio is assumed to be insensitive to the global electron momentum scale. The $e + 1$ jet sample contains $W \to e + \nu_e$ events associated with exactly one jet at the level of $\sim$80%. It was chosen for best balance between high statistics, moderate background from jets misidentified as electrons ("fake"electrons) and wide $E_{\rm T}$ range. The bottom plot of Figure 4 shows a linear fit of the data to MC E/P ratio as a function of $E_{\rm T}$ from which

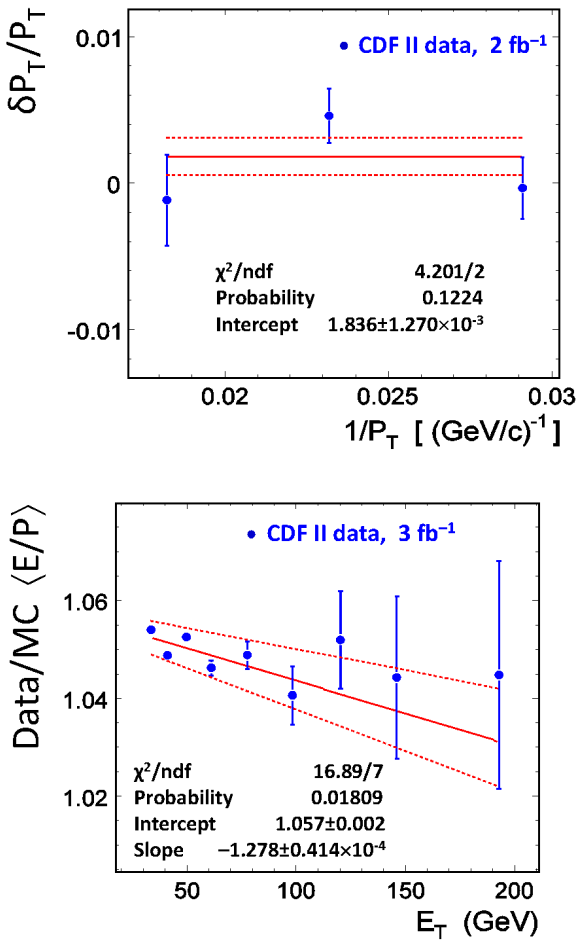

FIG. 4: **Top:** The constant term fit of the muon relative change of scale $\delta P_{\rm T}/P_{\rm T}$ as a function of $1/P_{\rm T}$ for $Z \to \mu^+\mu^-$ data. **Bottom:** The linear fit of the data to MC ratio of the electron average E/P over each $E_{\rm T}$ bin for $e+1$ jet data and MC. In each plot, the dashed lines represent $\pm 1\sigma$ variations of the respective fit.

the electron $E_{\rm T}$ calibration parameters are derived. Although moderately good, the fit suggests a decrease of the ratio with increasing $E_{\rm T}$, which can be attributed to energy leakage in the calorimeter. In both cases of muon and electron local scale, polynomial fits of higher degree yield coefficients of higher order terms of sizes well within the errors, having negligible effect on the calibration relative to the uncertainties of the fits shown in Figure 4.

The signal MC, based on the leading order (LO) PYTHIA generator, was also corrected for next-to-leading order (NLO) effects. The $t\bar{t}$ signal events were reweighted from the LO in α_s CTEQ5L [20] set of parton distribution functions (PDF) of the proton, which is the default in PYTHIA 6.2, to the NLO CTEQ6M set [21]. In addition, the LO 6% fraction of $gg \to t\bar{t}$ events of PYTHIA was scaled up to the NLO fraction of 15% [22] to provide a more accurate description of $t\bar{t}$ production.

The robustness of the method over the full range of

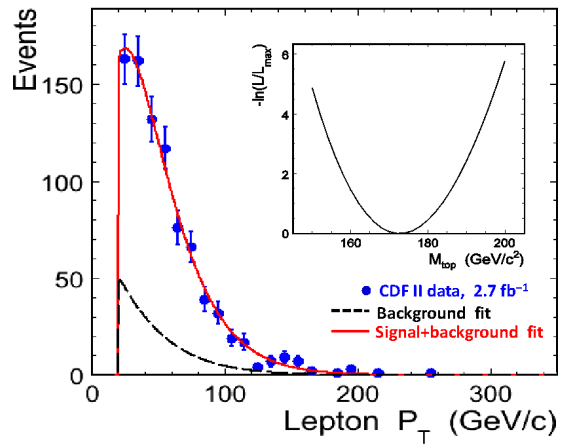

FIG. 5: The unbinned maximum likelihood fit of M_{top} to the data. The inset plot shows the log-likelihood curve of the fit. The result of the fit before any correction is $M_{top} = 171.9 \pm 7.9_{\rm stat}$ GeV/c^2.

M_{top} values covered by the MC signal templates was tested with simulated experiments, using in each experiment the number of events observed in the data and the expected sample composition of Table I. The signal and background events were randomly sampled for each experiment from the respective templates and a new fit was performed each time using the parameters of Table II and maximizing the likelihood defined by Equation 3. It was found in all cases that the method is unbiased and the statistical uncertainty of the measured M_{top} is correctly estimated. The expected relative statistical uncertainty is 4.5% after the lepton $P_{\rm T}$ scale corrections and the reweighting from LO to NLO PDF are applied.

VI. RESULT

A maximum likelihood fit was performed to the 2.7 fb^{-1} data sample consisting of 858 lepton+jets events, 472 of which are electron+jets events and 386 are muon+jets. The fit is shown in Figure 5 and the result is $M_{top} = 171.9 \pm 7.9_{\rm stat}$ GeV/c^2 before any corrections. The χ^2/n.d.f. of the fit is 21.4/27=0.79, corresponding to a χ^2 probability of 0.77. The total $P_{\rm T}$ scale correction shifts the result of the fit by +2.6 GeV/c^2. The total correction of the result for the NLO reweighting is +2.4 GeV/c^2. The two corrections add to an overall correction of +5.0 GeV/c^2 of the fit result to give a final result of $M_{top} = 176.9 \pm 8.0_{\rm stat}$ GeV/c^2, where the increase of 0.1 GeV/c^2 in the statistical uncertainty follows from the increase in the central value.

All systematic uncertainties are determined by performing simulated experiments in which the systematic parameter in question is varied, the default method and corrections are applied, and the shift in the average mea-

sured top quark mass with respect to the value measured from the nominal sample is used to quantify the uncertainty. The systematic uncertainties are summarized in Table III. The uncertainty from the finite MC statistics was estimated by varying the shape parameters of Table II by $\pm 1\sigma$. The uncertainty from the lepton $P_{\rm T}$ scale was estimated by varying the lepton $P_{\rm T}$ correction parameters by $\pm 1\sigma$ of the respective fit from which each parameter was derived. This uncertainty is sizeable and almost entirely originating from the local scale calibration where the information provided by the data is poor, as seen in Figure 4. An estimate of the uncertainty from the choice of the MC event generator was obtained by comparing the fit to the default PYTHIA $t\bar{t}$ sample with the fit to a HERWIG [23] $t\bar{t}$ sample, including the total background in both cases. The uncertainty from the proton PDF set was estimated by varying the CTEQ6M eigenvectors and the α_s value within their 90% errors. For the gluon initial and final state radiation, an estimate of the uncertainty was obtained by comparing the fits to two signal+background MC samples with higher and lower radiation with the fit to the default sample. For the multiple hadron interactions, the uncertainty was estimated by reweighting the default MC sample to the average number of vertices in the high instantaneous luminosity part of the data. For the background shape uncertainties, the uncertainty of the W+jets component due to the choice of the Q^2 scale was estimated by varying the Q^2 scale by a factor of 2 up and a factor of 2 down relative to the default, and the uncertainty due to the amount of fakes by varying the expected amount of fakes of Table I by $\pm 1\sigma$, while keeping the normalization of the total background fixed. The variation of the fakes fraction in the total background is $\sim$65% and affects the shape of the total background distribution to a degree consistent with the shape discrepancy between data and expectations in the lepton + 2 jets control sample for $P_{\rm T} < 50$ GeV/c, seen in Figure 1. This is the largest source of systematic uncertainty in this measurement. Finally, an estimate of the uncertainty from the jet energy scale was obtained by varying the combined jet energy corrections by $\pm 1\sigma$ [12] and it was found to be negligible. The total systematic uncertainty was estimated by adding all individual uncertainties in quadrature and was found equal to 2.7 GeV/c^2.

TABLE III: Systematic uncertainties of the measurement. All uncertainties are estimated at $M_{top} = 175$ GeV/c^2.

Source	Uncertainty (GeV/c^2)
MC statistics	0.4
Lepton $P_{\rm T}$ scale	1.1
MC generator	1.2
Proton PDF	0.6
Gluon radiation	0.8
Multiple interactions	0.1
Q^2 scale	0.5
Fakes	1.8
JES	negligible
Total	2.7

VII. SUMMARY AND CONCLUSIONS

In summary, the top quark mass was measured using a shape analysis of the lepton $P_{\rm T}$ distribution from a sample of 2.7 fb^{-1} of CDF II data. Events were selected in the lepton + $\geq$4 jets topology with at least one jet tagged as coming from a b quark. A MC derived model of the dependence of the lepton $P_{\rm T}$ distribution on M_{top} was used in an unbinned maximum likelihood fit to the data. Corrections for a detailed lepton $P_{\rm T}$ scale calibration and for NLO effects in the MC model of $t\bar{t}$ production were applied to the fit result in order to reduce systematic uncertainties from these two sources. Uncertainties from the jet energy scale are negligible. The dominant uncertainty was found to come from the shape model of the background, due to the large uncertainty in the expected fraction of fake electrons in the selected events. The final result is

$$M_{top} = 176.9 \pm 8.0_{\rm stat} \pm 2.7_{\rm syst}\ {\rm GeV}/c^2$$

in good agreement, within errors, with the current world average [24].

Compared with the previous measurement of exploiting the mean value of the lepton $P_{\rm T}$ with data corresponding to 1.9 fb^{-1} integrated luminosity in the lepton+jets channel [8], the new result shows an appreciable reduction, from 3.8 GeV/c^2 to 2.7 GeV/c^2, in the total systematic uncertainty. This is achieved by the use of the shape information of the lepton $P_{\rm T}$ distribution which is less sensitive to acceptance related effects that can change the mean $P_{\rm T}$ without altering significantly the shape of the $P_{\rm T}$ spectrum, such as the JES and multiple interactions, and by the new lepton $P_{\rm T}$ calibration, which reduced the $P_{\rm T}$ scale uncertainties.

Acknowledgments

We thank the Fermilab staff and the technical staffs of the participating institutions for their vital contributions. This work was supported by the U.S. Department of Energy and National Science Foundation; the Italian Istituto Nazionale di Fisica Nucleare; the Ministry of Education, Culture, Sports, Science and Technology of Japan; the Natural Sciences and Engineering Research Council of Canada; the National Science Council of the Republic of China; the Swiss National Science Foundation; the A.P. Sloan Foundation; the Bundesministerium für Bildung und Forschung, Germany; the Korean World

Class University Program, the National Research Foundation of Korea; the Science and Technology Facilities Council and the Royal Society, UK; the Institut National de Physique Nucleaire et Physique des Particules/CNRS; the Russian Foundation for Basic Research; the Ministerio de Ciencia e Innovación, and Programa Consolider-Ingenio 2010, Spain; the Slovak R&D Agency; and the Academy of Finland.

[1] F. Abe *et al* (CDF Collaboration), Phys. Rev. Lett. **74**, 2626 (1995); S. Abachi *et al* (D0 Collaboration), Phys. Rev. Lett. **74**, 2632 (1995).

[2] The Tevatron Electroweak Working Group, FERMILAB-TM-2427-E, arXiv:0903.2503v1.

[3] The LEP Collaboration, CERN-PH-EP/2007-039, arXiv:0712.0929v2.

[4] T. Aaltonen *et al* (CDF Collaboration), Phys. Rev. Lett. **105**, 252001 (2010); T. Aaltonen *et al* (CDF Collaboration), Phys. Rev. D **81**, 052011 (2009).

[5] W. M. Yao *et al*, "Review of Particle Physics", J. Phys. G **33**, 2006.

[6] N. Giokaris *et al* JINR-E1-2005-104, July 2005, p. 17.

[7] The transverse momentum $P_{\rm T} = P\sin\theta$ and transverse energy $E_{\rm T} = E\sin\theta$ of a particle are defined from its momentum P or energy E, respectively, and the polar angle θ of its momentum vector in a system of spherical coordinates with the polar axis along the proton beam. The pseudorapidity of the particle is given by $\eta = -\ln[\tan(\theta/2)]$.

[8] T. Aaltonen *et al* (CDF Collaboration), Phys. Rev. D **81**, 032002 (2010).

[9] CDF II Collaboration, FERMILAB-PUB-96/90-E (1996), and A. Abulencia *et al.*, J. Phys. G: Nucl. Part. Phys. **34**, 2457 (2007); see also A. Sill *et al.*, Nucl. Inst. Meth. **A447**, 1 (2000) and T. Affolder *et al.*, Nucl. Inst. Meth. **A425**, **86**, 249 (2004) for the tracker; L. Balka *et al.*, Nucl. Inst. Meth. **A267**, 272 (1988) and S. Bertolucci *et al.*, Nucl. Inst. Meth. **A267**, 301 (1988) for the central calorimeters.

[10] The missing transverse energy, measuring the transverse energy inbalance of the event, is defined by $\not\!\!E_{\rm T} = |\sum_{towers} E_{\rm T}\hat{n}_{\rm T}|$, where $\hat{n}_{\rm T}$ is the unit vector normal to the beam and pointing to a given calorimeter tower and $E_{\rm T}$ is the transverse energy measured in that tower.

[11] The calorimeter isolation is defined as the difference of the total $E_{\rm T}$ in a cone of radius $R = \sqrt{(\Delta\eta)^2 + (\Delta\phi)^2} = 0.4$ around the axis of a tower cluster minus the total $E_{\rm T}$ in the cluster, where ϕ is the azimuth in the spherical coordinate system.

[12] A. Bhatti *et al* (CDF Collaboration), Nucl. Inst. Meth. **A566**, 375 (2006).

[13] D. Acosta *et al* (CDF Collaboration), Phys. Rev. D **71**, 052003 (2005).

[14] T. Sjostrand, P. Eden, C. Friberg, L. Lombard, G. Miu, S. Mrenna and E. Norrbin, Comp. Phys. Comm. **135**, 238 (2001); the version of Pythia used here is 6.2.16.

[15] M. L. Mangano, M. Moretti, F. Piccinini, R. Pittau and A. Polosa, J. High Energy Phys. 07 (2003) 001.

[16] F. Maltoni, T. Stelzer, J. High Energy Phys. 02 (2003) 027.

[17] E. Gerchtein and M. Paulini, CHEP-2003-TUMT005, arXiv:physics/0306031 (2003); the version of Geant used for the detector simulation is 3.21, see the CERN Program Library Long Writeup W5013.

[18] D. Acosta *et al* (CDF Collaboration), Phys. Rev. D **71**, 072005 (2005).

[19] F. James, CERN Program Library Long Writeup D506, 1994.

[20] H. L. Lai, J. Huston, S. Kuhlmann, J. Morfin, F. Olness, J.F. Owens, J. Pumplin and W. K. Tung, Eur. Phys. J. C **12**, 375 (2000).

[21] J. Pumplin, D. R. Stump, J. Huston, H. L. Lai, P. Nadolsky and W. K. Tung, J. HEP **0207**, 012 (2002).

[22] S. Moch and P. Uwer, Nucl. Phys. Proc. Suppl. **183**, 75 (2008).

[23] G. Corcella, I. G. Knowles, G. Marchesini, S. Moretti, K. Odagiri, P. Richardson, M. H. Seymour and B. R. Webber, J. High Energy Phys. 01 (2001) 010.

[24] The CDF and D0 Collaborations, arXiv:1007.3178 (2010).